Application of a Hypergeometric Model in Simulating Canopy Gap Fraction and BRF for Forest Plantations on Sloping Terrains

Jun Geng, Jing M. Chen, *Senior Member, IEEE*, Weiliang Fan, *Member, IEEE*, Lili Tu, Yong Pang, Gang Yuan, Lichen Xu, Canyang Zhu, Teng Zhang, Chunju Zhang, Zhourun Ye, Yongchao Zhu, and Zhenxuan Li

***Abstract*—The influence of tree distribution and slope on canopy gap fraction (GF) and bidirectional reflectance factor (BRF) is shown here to be non-negligible. Trees are often assumed to be randomly distributed in natural forests due to random distribution of natural resources, but this assumption is not valid for forest plantations. A geometric optical model for forest plantations (GOFP) is a geometric optical model for forest plantations on horizontal surfaces based on the theory of exclusion distance among crowns. Sloping terrains change the exclusion distance among crowns, and inevitably affect the canopy GF and BRF. In this article, GOFP with a hypergeometric model (distances among trees are considered) on horizontal surfaces is modified as GOFP-T to simulate BRF for forest plantations on sloping terrains under two scenarios: (horizontal distances among crowns remain unchanged with slope) and (sloping distances among crowns remain unchanged with slope). Two three-dimensional (3-D) radiative transfer models (DART and LESS) and field measurements are used to evaluate and validate GOFP-T simulations. The results show that 1) the canopy GF, four component area ratios, and canopy BRF simulated by GOFP-T show high consistency with results from the two 3-D model: root-mean-square errors in GF, sunlit foliage, and sunlit ground are less than 0.02, 0.06, and 0.03, respectively; 2) forest coverage and canopy reflectance in GOFP-T are compared well with point cloud results from an airboard LiDAR system and Landsat 8 OLI surface reflectance products, respectively, indicating that GOFP-T has ability in simulating canopy reflectance for forest plantations on sloping terrains. GOFP-T with the hypergeometric model in this article is the first simple model to simulate canopy GF and BRF for forest plantations on sloping terrains.**

***Index Terms*—Bidirectional reflectance factor (BRF), forest plantation, gap fraction (GF), GOFP-T, hypergeometric model, sloping terrain.**

Manuscript received September 9, 2021; revised December 27, 2021 and February 13, 2022; accepted March 1, 2022. Date of publication March 7, 2022; date of current version April 21, 2022. This work was supported in part by the National Natural Science Foundation of China under Grant 41701383 and Grant 41801234 and in part by the Anhui Provincial Natural Science Foundation under Grant 1808085QD105. *(Corresponding author: Lili Tu.)*

Jun Geng, Gang Yuan, Lichen Xu, Canyang Zhu, Teng Zhang, Chunju Zhang, Zhourun Ye, Yongchao Zhu, and Zhenxuan Li are with the School of Civil Engineering, Hefei University of Technology, Hefei 230009, China, and also with the Intelligent Interconnected Systems Laboratory of Anhui Province, Hefei University of Technology, Hefei 230009, China (e-mail: gaoyugengjun@163.com; 2020110660@mail.hfut.edu.cn; lichenxu@mail.hfut.edu.cn; 2019170621@mail.hfut.edu.cn; 2021110630@mail.hfut.edu.cn; zcjtwz@sina.com; yezhourun329@hotmail.com; yczhu@hfut.edu.cn; cehuilzx@126.com).

Jing M. Chen is with the Fujian Normal University, Fuzhou 350000, China, and also with the Department of Geography and Program in Planning, University of Toronto, Toronto, ON M5S 3G3, Canada (e-mail: jing.chen@utoronto.ca).

Weiliang Fan is with the College of Environmental and Resource Sciences, Zhejiang A&F University, Linan 311331, China (e-mail: fanweiliang@163.com).

Lili Tu is with the School of Resources and Environment, Anhui Agricultural University, Hefei 230009, China (e-mail: tulili@ahau.edu.cn).

Yong Pang is with the Institute of Forest Resource Information Techniques, Chinese Academy of Forestry, Beijing 100091, China (e-mail: pangy@ifrit.ac.cn).

Digital Object Identifier 10.1109/JSTARS.2022.3156403

I. Introduction

TREE distribution pattern plays a vital role in forest succession, regeneration, growth, and understory development [1]–[4]. It has been shown to influence forest coverage, directional canopy gap fraction (GF), canopy four component area ratios (sunlit leaves, shaded leaves, sunlit background, and shaded background), and bidirectional reflectance factors (BRF) [5], [6]. The Poisson model is most frequently used in many canopy bidirectional reflectance distribution function (BRDF) models based on the assumption of randomness of natural resources, i.e., water, nutrient, and soil depth [7]–[11]. Trees in forest plantations are planted by human often in regular patterns to maintain enough space for trees to grow and develop. The assumption of random distribution of trees in the Poisson model is invalid for forest plantations [5], [6]. The Poisson model allows the probability of overlaps among crowns, but crowns seldom overlap in competition for light and maintain mutually exclusion distances from each other in reality. As the Poisson model cannot describe the exclusion distance among trees in forest plantations, some more sophisticated models have been used to describe tree distributions, and there have been studies on the effects of tree distribution on canopy GF and BRF. For instance, Chen and Leblanc used a Neyman-A model to consider the effect of tree grouping in natural forests on BRF [12]. An empirical exclusion distance among crowns was added into a canopy BRDF model to show the regularity of tree distribution in a forest stand [13]. Nilson [14] and Kuusk *et al.* [15], [16] described tree distributions in canopy BRDF models based on statistic parameters (e.g., variance). Some more complicated models have been used to describe the tree distributions in a stand, e.g., the hybrid-Gibbs point processes [17]. These models need accurate tree positions and variance of tree number in a stand and inevitably increases their complexity. Tree distributions in forest plantations show obvious different spatial patterns from those in natural forests. Considering both randomness and regularity

This work is licensed under a Creative Commons Attribution 4.0 License. For more information, see https://creativecommons.org/licenses/by/4.0/

of tree distribution with a hypergeometric model, Geng *et al.* [5], [6] calculated canopy GF for forest plantations. In the model, a simple distance parameter (relatively allowable shortest distance among crowns, RASD) was used to quantitatively describe the exclusion distance among crowns arranged in regular patterns on horizontal surfaces [6]. Recently, the hypergeometric model was combined with a GOST2 model [18], and a geometric optical model for forest plantations (GOFP) was employed to simulate canopy GF, four component area ratios, and BRF on horizontal surface [5]. GOFP has been validated in describing tree distributions for forest plantations with *in situ* measurements, and simulating canopy GF, four component area ratios, and BRF using high-resolution images acquired at multiple angles on a UAV platform, and several stands on radiation transfer model intercomparison (RAMI) platform on horizontal surfaces [5], [19].

The influence of terrain slope on canopy GF and BRF has been studied extensively [20]–[23], [25], [27]. Canopy BRDF models for horizontal surfaces could be applied to sloping terrains after rotating the coordinate system [24]. This operation may not be correct in many cases because the geotropism of trees (i.e., trees always grow vertically rather than perpendicular to the sloping surfaces) was neglected [7], [25]. Although the tree geotropic nature has been widely accepted now, there are still two different trees-on-slope models being used: 1) horizontal distances among crowns do not change with increasing slope (HM) [20]–[23]; 2) slope distances among crowns do not change with increasing slope (SM) [26], [27].

Geometric optical (GO) models emphasize on the geometric structure of objects. Accurate calculation of overlaps among objects (e.g., crowns) is one of key steps in nearly all GO models. Both tree distribution and slope inevitably change the exclusion distance and overlaps among crowns, and then inevitably affect the canopy GF and BRF. However, up to now, no GO models are suitable for simulating canopy BRF for forest plantations on sloping terrains.

The aim of this article is to apply the hypergeometric model to simulate canopy BRF for forest plantations on sloping terrains. First, the theory of the hypergeometric model for forest plantations on sloping terrains is described in detail, and GOFP with the hypergeometric model for horizontal surfaces is modified to form GOFP-T for simulating canopy GF and BRF for forest plantations on two trees-on-slope models (HM and SM). Meanwhile, GOFP-T is evaluated with two three-dimensional (3-D) radiative transfer models. This article is organized as follows: the theories of calculating canopy GF, four scene component area ratios, and BRF for forest plantations on sloping terrains are described in detail in Section II; simulations of GOFP-T, GOST2, DART, LargE-Scale remote sensing data and image simulation framework (LESS), and field measurements are compared in Section III; the two trees-on-slope models are discussed in Section IV.

II. Theory and Methods

A. Canopy GF in the Poisson Model

1) Horizontal Surfaces: The Poisson model assumes that trees are randomly distributed in a stand without any exclusion effect [see Fig. 1(a)]. All crowns in the stand are independent to each other. For a canopy with opaque crowns, GF (P) of the canopy with a random tree distribution can be described as follows [12]:

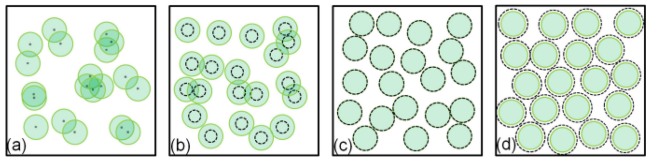

Fig. 1. Illustration of different exclusion area among crowns using a simple distance parameter RASD describing the relative allowable shortest distance between centers of two adjacent crowns divided by the mean diameter of the crowns (green discs mean crowns, and black circles mean crust (from (a)–(d), RASD $= 0$, $0 <$ RASD < 1, RASD $= 1$, and RASD > 1, respectively).

$$P_{Poi}(\theta) = \left[1 - \frac{cp(\theta)}{S \cdot \cos\theta}\right]^n \tag{1}$$

where $c_p(\theta)$ is the crown projection area in the view direction (θ) (subscript "p" means projection in the view), and can be calculated in geometry. S is the stand area on horizontal ground. [$S\cdot \cos(\theta)$] means the stand projection area in the direction θ. n is the number of trees in the stand.

For a canopy with porous crowns, GF within an individual crown needs to be considered. Canopy GF can be calculated as follows [6]:

$$P_{Poi}(\theta) = \left[1 - \frac{c_p(\theta) \cdot (1 - P_c(\theta))}{S \cdot \cos\theta}\right]^n \tag{2}$$

where $P_c(\theta)$ is the crown GF in the direction θ. It is a modification of Beer–Lambert's law, and closely related with the crown size, and leaf area in an individual crown. It can be calculated as follows [22]:

$$P_c(\theta) = \mathrm{e}^{-L_c \cdot G(\theta) \cdot \Omega_c / c_p(\theta)} \tag{3}$$

where L_c is the leaf area in an individual crown, $L_c / c_p(\theta)$ means the leaf area index in an individual crown in direction θ. G(θ) is the projection of unit leaf area in the direction θ and is equal to 0.5 for the spherical leaf angular distribution. Ω_c means the clumping index at scales larger than shoot in a crown. $\Omega_c = 1$ if leaves are assumed to be randomly distributed in a crown.

2) Sloping Terrains: For sloping terrains, the main difference from the horizontal surface is projection. As the crown projection $c_p(\theta)$ in the view direction θ does not change because of the geotropic nature of tree growth, the only difference for sloping terrains is the slope projected projection area in the view direction θ. Then, canopy GF on sloping terrains (P_T) can be calculated as

$$P_T(\theta) = \left[1 - \frac{cp(\theta) \cdot (1 - P_{\text{gap}}(\theta))}{Sp(\theta)}\right]^n \tag{4}$$

where $S_p(\theta)$ is the projection of stand area on the sloping surfaces in the view direction θ [22].

B. Canopy GF in the Hypergeometric Model

It is worth noting that the tree number (n) is allowed to be infinite in the Poisson model: canopy GF is close to 0 but always larger than 0 with the increment of tree number in (1)–(4).

This is unpractical because there must be a maximum tree number in a finite area. The primary reason of allowing the tree number to be infinite is that crowns are independent to each other and are randomly distributed in a stand in the Poisson model. It is like a random sampling with replacement and the sample size can be infinite. The hypergeometric model is developed to solve this problem of the infinite tree number. It is a random sampling without replacement. Besides randomness, there must be an exclusion distance among crowns and a maximum tree number in a stand. Geng *et al.* [6] applied the hypergeometric model in describing tree distributions and calculating canopy GF for forest plantations on horizontal ground surfaces. They deemed that each crown needs to occupy a private space (like a crust or core for each crown), which is not allowed to be occupied by any other crowns when viewed from nadir. For forest plantations, the assumption in the hypergeometric model is more reasonable than in the Poisson model. The reliability of the hypergeometric model has been validated *in situ* measurements in several forest plantation stands [5], [6], [19].

1) Horizontal Surfaces: A simple distance parameter defined as the relative allowable shortest distance between centers of any two crowns divided by the mean diameter of the crowns on horizontal surfaces (RASD) in the hypergeometric model was used to describe the degree of the exclusion effect among crowns in forest plantations. Fig. 1 shows different exclusion areas among crowns on horizontal surfaces at nadir (green discs mean crowns, and black circles mean crown crust (crown private area cannot be overlapped by other crown private area). In Fig. 1(a), RASD and crusts are nearly equal to zero, meaning trees are randomly distributed in a stand; from Fig. 1(a) to (d), RASD $=0, 0<$ RASD <1, RASD $=1$, and RASD >1, respectively, and the crust size increases with RASD. Although the tree numbers in the four stands are identical in Fig. 1, forest coverage and canopy GF are obvious different. In most cases, the shortest distance among crowns is close to crown diameter, meaning the nearest two crowns in the stand is tangent and RASD is nearly equal to 1.

Different from the Poisson model, canopy GF in the hypergeometric model can be described as follows [6]:

$$P_{Hyp}(\theta) = \prod_{j=1}^{i}\left[1-\frac{c_p(\theta)\cdot(1-P_c(\theta))}{S\cdot\cos\theta - S_{\text{real\_excl\_}p}(\theta)\cdot(1-P_c(\theta))\cdot(j-1)}\right] \tag{5}$$

where $S_{\text{real\_excl\_}p}(\theta)$ is the real exclusion area projected in the view direction θ. ("real" will be explained later). After plotting *j*th tree crown in the stand, canopy GF is the accumulation of results. The only difference between the hypergeometric and the Poisson model is the denominator in (5). There is a maximum of crown number in the stand. When the crown number exceeds the maximum allowable value, the denominator in (5) will be equal to or less than zero; and then, GF will be equal to or less than 0, which is unrealistic.

It is worth noting that the real exclusion projection area $S_{\text{real\_excl\_}p}(\theta)$ is not always equal to the crust projection area $S_{\text{crust\_}p}(\theta)$. It is due to that blank region [blue oblique lines in Fig. 2(b) and (c)] inside of a crust but outside of a crown needs be deducted when calculating canopy GF. For instance, the canopy GFs at nadir in Fig. 1(c) and (d) are identical, although RASD and the crust area are different between these two stands. In the hypergeometric model, the abovementioned deducted parts call the "pseudo" region. It is related with both the crust and crown projected areas in the view direction, and can be calculated in geometry. Then, the $S_{\text{real\_excl\_}p}(\theta)$ can be expressed as follows:

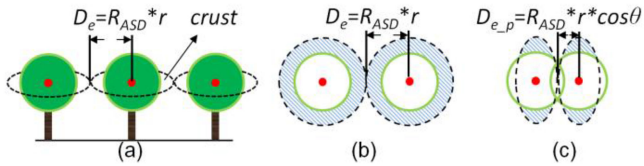

Fig. 2. Illustration of the spatial relationship among crowns in the hypergeometric model for forest plantations on horizontal surfaces (dotted ellipses mean crust or core for each crown. Blue oblique lines mean the "pseudo" exclusion area. (a) Exclusion distance (D_e) and crust area (S_{crust}) in a forest plantation stand. (b) D_e and S_{crust} projected on the view plane at VZA $=0°$, then crust area projection is a circle. (c) D_e and S_{crust} projected on the view plane (D_{e_p} and S_{crust_p}) at VZA $>0°$, then crust area projection is a ellipse because of the decrement of projected exclusion distance in the view direction).

$$S_{\text{real\_excl\_}p}(\theta)=S_{\text{crust\_}p}(\theta)-S_{pse\_p}(\theta). \tag{6}$$

If view zenith angle (VZA) $=0°$, the crust area projection in the view direction is a circle [see Fig. 2(b)]. If VZA $\neq 0°$, the projection in the view direction in (5) is not a circle but an ellipse [the semi-axis of ellipse parallel with θ will decrease in Fig. 2(c)]. The main difference between the Poisson model and the hypergeometric model is the exclusion area for each crown [denominator in (5)]. For additional information about the hypergeometric model, please refer to [6].

2) Sloping Terrains: Essentially, the modification of canopy GF from horizontal surfaces to sloping terrains is actual a projection transformation. For the Poisson model, the modification is simple [from (2) to (4)]. Yet, it is not straightforward for the hypergeometric model because of its dependence on tree distributions. Slope changes the crust and crown projected areas, overlaps and the exclusion distances among crowns in the view direction, and therefore, it must change the real exclusion projection area of crowns in (5). Two trees-on-slope models have been widely used in many BRDF models.

1) Parameters projected on horizontal surfaces do not change with slope: the horizontal distance among trees, the number of trees, leaf area index, and the vegetation coverage remain unchanged with slope; yet, the sloping distance among trees and slope area increase with increasing slope. Here we call it HM.
2) Parameters on sloping terrains do not change with slope: the sloping distances among trees, leaf area on sloping surface do not change with slope; while vegetation cover increases with increasing slope. Here, we call it SM.

HM is a more common used scenario than SM in literature [18], [22], [28], especially for natural forests. Yet, the optimal strategy of forest management is to make maximum use of space on slope surfaces for forest plantations. More trees can

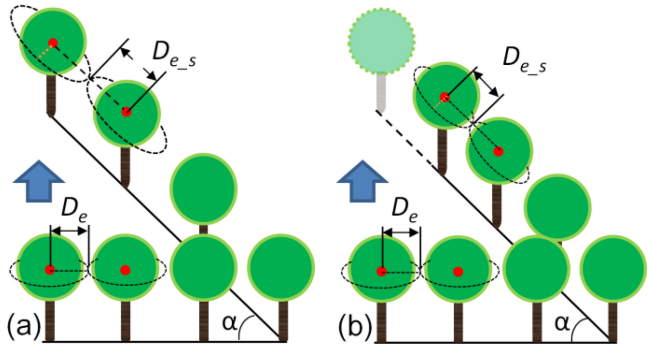

Fig. 3. Illustration of exclusion distances among crowns in forest plantations on two different models (D_e means exclusion distance among crowns on horizontal surfaces; D_{e_s} means exclusion distance among crowns along slope on sloping surfaces. (a) HM: the horizontal parameters remain unchanged, but the sloping distance increases with slope, and $D_{e\_s} > D_e$. (b) SM: the slope parameters remain unchanged, and $D_{e\_s} = D_e$).

be planted in SM on the same area of a sloping surface with HM [e.g., extra crowns can be planted on a sloping surface (about 44°) in SM (the semitransparent crown in Fig. 3(b))]. The difference in the distances among crowns between these two trees-on-slope models inevitably leads to the difference in the directional canopy GF. In this article, both trees-on-slope models are adopted to show how the exclusion distance among crowns affect canopy GF and BRF on sloping terrains. Then, we rewrite (5) as the following equation:

$$P_{s\_Hyp}(\theta) = \prod_{j=1}^{i} \left[1 - \frac{c_p(\theta) * (1 - P_c(\theta))}{S_p(\theta) - S_{s\_\int \text{real\_excl}\_p}(\theta) * (1 - P_c(\theta)) * (j-1)}\right] \tag{7}$$

where $S_{s\_\text{real}\_\text{excl}\_p}(\theta)$ means the projection of real exclusion area on slope terrains in θ. Some variables are different in (7) between HM and SM.

1) For HM: the exclusion distance among crowns along slope $D_{e\_x} = D_e/\cos(\alpha)$; curst area on slope $S_{\text{curst}\_x} = S_{\text{curst}}/\cos(\alpha)$; curst area on slope projected in the view direction $S_{\text{curst}\_x\_p} = S_{\text{curst}\_x}/\cos <\text{F}_{\text{view}}, \text{F}_{\text{slope}}>$. Where, F_{view} and F_{slope} mean the view and slope normal vector, respectively. $<\text{F}_{\text{view}}, \text{F}_{\text{slope}}>$ is the angle between these two vectors. Combined with the crown projected area $c_p(\theta)$ in the view direction, then real exclusion area on slope projected in the view direction $S_{\text{real}\_\text{excl}\_p}(\theta)$ can be calculated using (6).
2) For SM: the crust area (S_{crust}) on slope does not change with slope. While both crust and crown projection areas [$S_{\text{crust}\_p}(\theta)$ and $c_p(\theta)$] in the view direction θ change with slope, leading to the real exclusion area in the view direction θ [$S_{\text{real}\_\text{excl}\_p}(\theta)$] also change with slope.

After constructing the HM and SM models, we modify GOFP with the hypergeometric model for horizontal surfaces to form GOFP-T for sloping terrains. The main difference between GOFP and GOFP-T is the variation of crust projection area and real exclusion projection area in the view direction with slope. As the real exclusion projection area is an intersection between the crown projection and crust projection [as shown in Fig. 2(c)], the specific calculations are not given here.

C. Four Component Area Ratios

For GO models, four component area ratios are key intermediate variables for canopy BRF. In the view direction, the stand scene can be separated into two components: foliage and ground. The latter is canopy GF (P). Similarly, the stand scene viewed from the sunlight direction (hotspot) can be separated into another two components: sunlit foliage and sunlit ground. Considering view and sunlight directions, the scene can be separated into four components in the view direction: sunlit foliage K_T, sunlit ground K_G, shaded foliage K_{ZT}, and shaded background K_{ZG}. Except for the particular VZA (i.e., at the hotspot), these four components all have contributions to the whole field of view. The ability of GOFP and GOST2 in simulating the four components area ratios for natural forests has been validated in previous studies [5], [7], [18]. The separations of K_G from seeing ground (P) and K_T from seeing foliage ($1 - P$) in GOFP-T are similar to those in GOST2

$$KG = PigPvg + (Pig - PigPvg)Ft(\xi) \tag{8}$$

where P_{ig} and P_{vg} is the gap fraction in the sunlight and view directions, respectively. $F_t(\xi)$ is the hotspot function [22]. Then, the shaded background in the view direction is calculated as: $K_{ZG} = P - K_G$. The main differences between GOFP-T and GOST2 exist in canopy gap fractions in both view and sun directions. The equation for separating K_T and K_{ZT} for forests on slope terrains is not explicitly given here. In GOFP-T, this separation is made through a ray-tracing method, following the method used in GOFP [5].

D. Canopy Reflectance

The spectral reflectance of forest canopies is composed of four scene components: sunlit foliage (K_T), sunlit ground (K_G), shaded foliage (K_{ZT}), and shaded ground (K_{ZG}). Each proportion is multiplied by its reflectivity factor that depends on the wavelength used. Then, the canopy reflectance can be calculated as follows:

$$R = R_T * K_T + R_G * K_G + R_{ZT} * K_{ZT} + R_{ZG} * K_{ZG} \tag{9}$$

where R_T, R_G, R_{ZT}, and R_{ZG} are the reflectivity factors of the K_T, K_G, K_{ZT}, and K_{ZG} in GOFP-T, respectively.

III. Methods

Developed since 1992, (Discrete Anisotropic Radiative Transfer (DART),[1] which is a 3-D radiation interaction model, has been successfully applied to simulating canopy BRF and the spectral radiation budget of many natural objects (e.g., trees, grass, and soil) and artificial objects (e.g., building and road) in the visible and short wave infrared spectral domains [29], [32]. Its accuracy has already been tested for simulating vegetation canopy directional reflectance (RAMI experiments,[2] *in situ* and

[1] [Online]. Available: https://dart.omp.eu
[2] [Online]. Available: https://rami-benchmark.jrc.ec.europa.eu

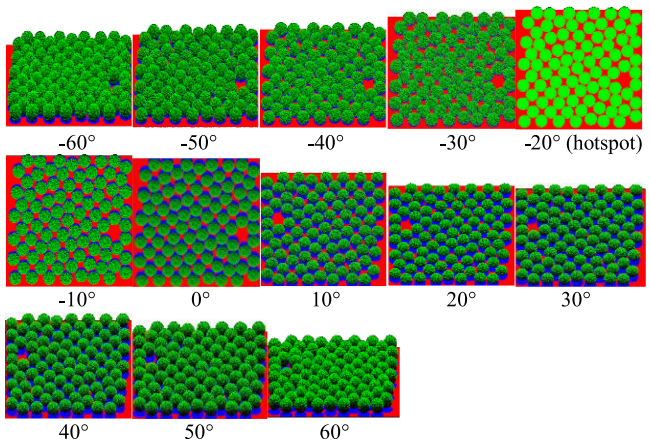

Fig. 4. Four component area ratios on the principal plane separated in LESS at different VZAs (Green: sunlit foliage; red: sunlit background; black: shaded foliage; blue: shaded background. For rapid calculation, only 1/25 of the stand (400 m^2) with 88 tree crowns is simulated. Negative VZAs mean the relative view azimuth angle between sun and view is 0°, and positive VZAs mean the relative azimuth between sun and view is 180°).

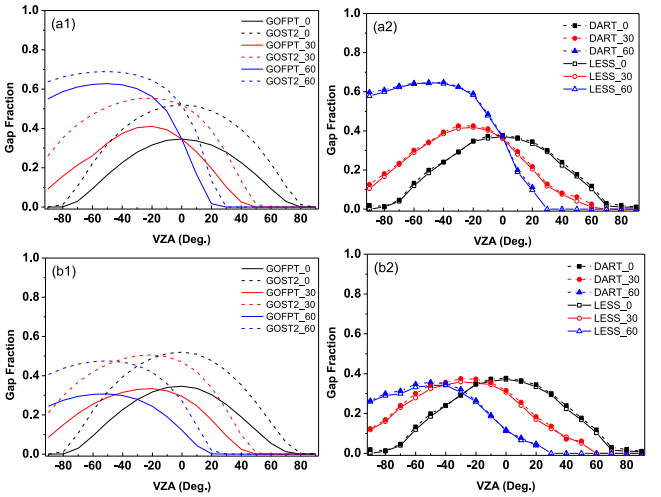

Fig. 5. Comparisons of GF among GOFP-T, GOST2, DART, and LESS on the principal plane on the two trees-on-slope models with slope = 0°, 30°, and 60°, respectively [(a) HM and (b) SM; (1) two GO model results and (2) two 3-D model results]. [Negative VZAs mean the relative azimuth angle between sun and view is 0° (in the backward-scattering direction), and positive VZAs mean the relative azimuth between sun and view is 180° (in the forward-scattering direction)].

airborne data) [26], [34]–[36]. DART does not directly produce the four components in a specific observation direction. The flexibility of DART allows one to compute the four components after some manipulations of its first-order scattering image products for individual scene element (i.e., an image product that stores only the emitted or scattered radiation from a predefined scene element such as foliage or ground). The foliage surface is computed from the brightness temperature image of foliage since no shadow appears in brightness temperature image. The sunlit foliage surface is computed from the optical reflectance image of foliage since the shadow reflectance is zero in the first order scattering. The difference of the two is the shadow foliage surface. The sunlit ground and shadow ground components can be derived similarly [29].

A 3-D radiative transfer simulation framework LESS (large-scale remote sensing data and image simulation framework over heterogeneous 3-D scenes,[3] which operates in both forward and backward model and can accurately simulate multispectral, multiangle images and radiation properties of realistic landscapes. It has been validated with field measurements and compared well with other models from the RAMI experiment. Moreover, LESS provides an additional Python tool to batch the classifications of the four component area ratios in multiple directions rapidly, which greatly improves the computational efficiency of the classifications at multiple VZAs [31], [37]–[38].

In this article, canopy GFs are simulated by the two GO models (GOFP-T and GOST2) and two 3-D radiative transfer models (DART and LESS) on the principal plane in the two trees-on-slope models (HM and SM) with three degrees: 0° (horizontal surface), 30° (medium slope), and 60° (steep slope), respectively (see Fig. 5). Two kinds of VZA are used in the article: 1) VZA, also called the global VZA, and the reference is the normal vector of horizontal surface; 2) local VZA, and the reference is the normal to the sloping surface. Negative VZAs mean the relative azimuth between sun and view is 0°, and positive VZAs mean the relative azimuth between sun and view is 180°.

TABLE I
INPUT PARAMETERS IN THE MODELS

Parameter	Value
Crown radius (m)	1
Crown height (m)	2.5
Height of the lower part of the tree (trunk space) (m)	0.5
LAI for slope = 0°*	4
Tree density for slope = 0° (trees/ ha)	2200
Crown shape	Ellipsoid
Leaf angle distribution	Spherical
RASD for slope = 0° (m)	0, 1
Vegetation coverage for slope = 0° (%)	69
Sun zenith angle (°)	20
Sun azimuth angle (°)	0
Slope (°)	0, 30, 60
Slope azimuth angle (°)	0
R_T (red, NIR)	0.05, 0.55
T_T (red, NIR)	0.1, 0.3
R_G (red, NIR)	0.15, 0.18

*For other slopes, parameters need to be recalculated according to trees-on-slope model and slope. TT means foliage transmittance.

The input parameters in reasonable ranges are listed in Table I. In addition, vegetation and background optical parameters are set to reasonable values, e.g., R_T is less than R_G in the red band; while R_T is larger than R_G in the NIR band. Some assumptions are made, including: the leaf angles are spherically distributed, and leaves are randomly distributed in an individual crown. These assumptions are commonly used in literature [7], [15], [18], [22], [28], [30], [39].

The 3-D virtual scenes models and software have been widely used to validate the canopy GF and four component area ratios.

[3][Online]. Available: http://lessrt.org

Some virtual software (e.g., 3-D Max) provides a camera for simulating remote sensor. Images in each view direction can be recorded in camera. Then, canopy four component area ratios can be separated based on image classification methods. While, the camera field of view in 3-D Max inevitably affect the classification results, especially for pixels at the edges of images. The orthographic projection is used in two 3-D radiative transfer models (different from the perspective projection used in 3-D Max), meaning that all VZAs of pixel in an image are identical. The orthographic projection is corresponding to GOST2 and GOFP-T, and it is an ideal platform to validate canopy GF and four component area ratios in models, which have not considered the field of view. The canopy on horizontal surfaces is separated into four components on the principal plane (see Fig. 4).

IV. Results

A. Canopy GFs

As shown in Fig. 5, for horizontal surfaces, the curves of GF are symmetrical between in the up-slope and down-slope directions. With increasing slope, all GF curves reach up to the maximum in the direction perpendicular to the slope surface (i.e., at local VZAs $= 0°$). It is due to that the projection area of the stand on sloping surfaces reaches to the maximum in this direction. There is no obvious difference of GFs between DART and LESS. Taking LESS results for example, GF simulated with GOFP-T ($\mathrm{GF_{GOFPT}}$) show high consistency with those in LESS ($\mathrm{GF_{LESS}}$) at most VZAs. The root-mean-square error (RMSE) in GF between GOFP-T and LESS is only 0.02. The relative error between $\mathrm{GF_{GOFPT}}$ and $\mathrm{GF_{LESS}}$ ($(\mathrm{GF_{GOFPT}} - \mathrm{GF_{LESS}})/\mathrm{GF_{LESS}}$) are less than 10% at most VZAs. However, GF simulated by GOST2 ($\mathrm{GF_{GOST}}$) show obvious deviations from LESS simulations. RMSE in GF between GOST2 and LESS reaches up to 0.12. The relative error between $\mathrm{GF_{GOST}}$ and $\mathrm{GF_{LESS}}$ reaches up to 40% at nadir. With the increment of VZA, the relative error in the Poisson model increases substantially. It reaches up to 150% at VZA $= -50°$ for a horizontal surface, indicating that GF is seriously overestimated in GOST2.

The influence of tree distribution on canopy GF shows strong dependence on slope. GF shows different trends between the two trees-on-slope models (HM and SM) with increasing slope. GF decreases with increasing slope in the up-slope direction in both HM and SM. It is due to that the sloping surface projection area in the view direction decreases and the path length of light penetrating the canopy increases in the up-slope direction. GF decreases to zero when the view direction is parallel with the sloping surface (local VZA $= 90°$, and global VZA is equal to $90° -$ slope). However, GF increases significantly in the down-slope direction for HM with increasing slope, but decrease slightly for SM. It is due to that the mean distance among crowns on slope increases obviously for HM but remains unchanged for SM. The shapes of GF curves with three slopes are similar to each other for SM because of the crown shape is similar to sphere. Considering the crown height (2.5 m) is larger than its horizontal dimension (2 m), crown projection area in non-nadir direction is larger than that at nadir, leading to that GF on sloping terrains are lower than those on horizontal surfaces [see (5)].

The different variation in GF between HM and SM leads to the different variations of RMSE and relative errors. For the medium slope (30°), the RMSE and relative error in GF between GOST2 and LESS are also non-negligible for both trees-on-slope models: RMSE is 0.16 for HM, and 0.14 for SM; mean relative error reaches up to 60% for HM and 53% for SM. While for the steep slope (60°), RMSE is 0.14 for SM but only 0.07 for HM; mean relative error is 56% for SM, but only 27% for HM. It means that the difference between $\mathrm{GF_{GOST}}$ and $\mathrm{GF_{LESS}}$ decreases on the steep slope at the negative VZAs (in the down-slope direction) in HM. It is due to that the crown density and canopy coverage decrease obviously on the steep sloping surface, leading to the influence of exclusion distance among crowns on GF decrease for HM with the steep slope. It is not hard to understand: if there is only few (i.e., only one) crown in a stand, canopy GF is seldom affected by the tree distribution.

Overall, GFs simulated by GOFP-T are validated by DART and LESS: the relative errors between GOFP-T and two 3-D models are less than 10% at most VZAs, and RMSE are less than 0.02 on three slopes. While GF simulated by GOST2 is overestimated at most VZAs for both trees-on-slope models, especially for SM. The relative errors between $\mathrm{GF_{GOST}}$ and $\mathrm{GF_{LESS}}$ for SM are larger than 40% at most VZAs. With increasing slope, the relative errors between $\mathrm{GF_{GOST}}$ and $\mathrm{GF_{LESS}}$ for HM decrease on the steep slope at the negative VZAs, while they are also obvious on the steep slope at the negative VZAs.

B. Canopy Four Component Area Ratios

Canopy four component area ratios directly affect the canopy BRF, and therefore, they should be evaluated before canopy BRF be evaluated. The stand scene is separated into four components in DART and LESS (see Fig. 4): sunlit foliage (K_T), shaded foliage (K_G), sunlit background (K_{ZT}), and shaded background (K_{ZG}). Comparisons of four component area ratios among GOFP-T, GOST2, DART, and LESS are shown in Fig. 6 (HM) and Fig. 7 (SM). As canopies on horizontal surfaces in HM and SM are identical, simulations on horizontal surfaces for SM are not shown in Fig. 7.

As the reflectance factors of sunlit foliage (R_T) and sunlit background (R_G) are generally much larger than those of shaded foliage (R_{ZT}) and shaded background (R_{ZG}), canopy BRFs are mainly affected by the contributions of sunlit foliage and sunlit background. We focus on the comparisons of simulations of K_T and K_G among the four BRDF models. From Figs. 6 and 7, the shape and magnitude of four component area ratios are simulated well by GOFP-T. K_T and K_G simulated by GOFP-T are consistent with DART and LESS simulations, especially for K_G. RMSE in K_T and K_G between GOFP-T and two 3-D models are less than 0.06 and 0.03, respectively, on three slopes (0°, 30°, and 60°) in both HM and SM. While, the differences in both K_T and K_G between GOST2 and two 3-D models are obvious at most VZAs for SM. For HM, RMSE in K_G between GOST2 and the two 3-D models (DART and LESS) is 0.18 and 0.17 for the horizontal surface, 0.18 and 0.17 for the medium slope, and 0.16 and 0.15 for the steep slope. For SM, RMSEs in K_G between GOST2 and the two 3-D models is 0.18 and 0.19 for

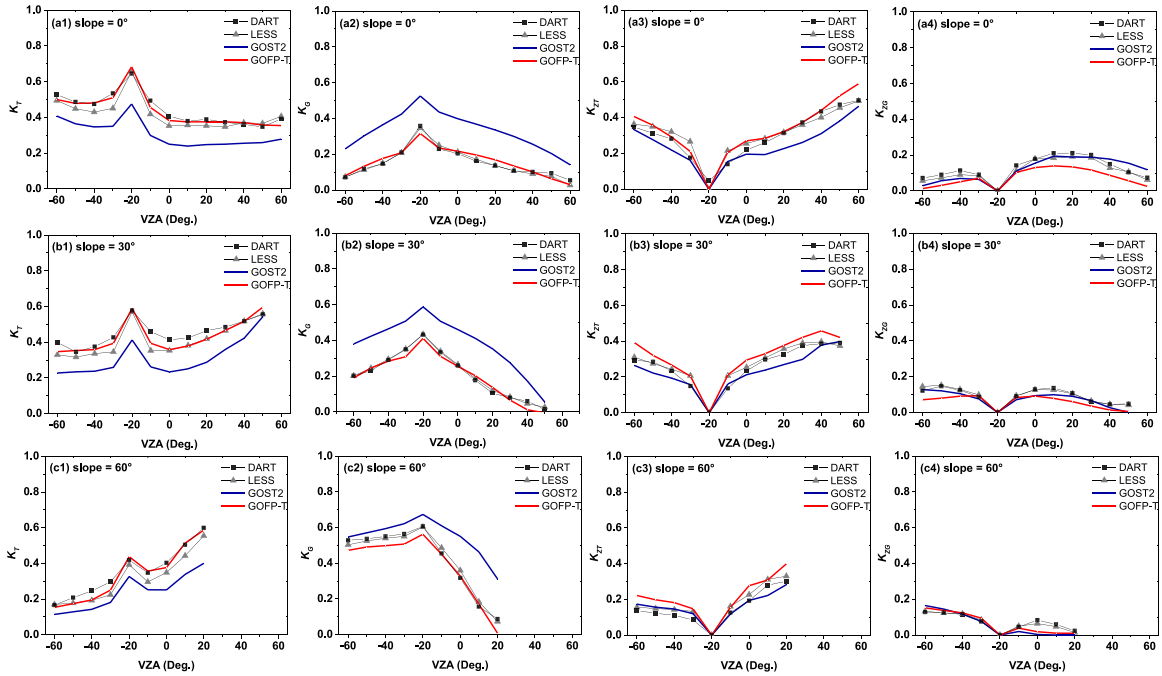

Fig. 6. Comparisons of four component area ratios among four BRDF models in HM with slope $=$ 0° (a), 30° (b), and 60° (c), respectively ((1) $K_{T,}$ (2) K_G, (3) K_{ZT}, and (4) K_{ZG}).

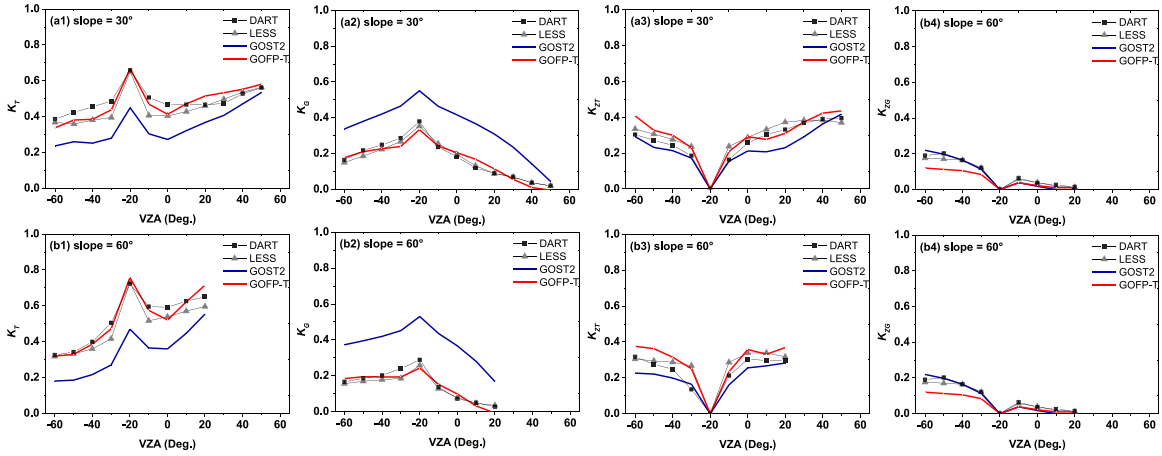

Fig. 7. Comparisons of four component area ratios among four BRDF models in SM with slope $=$ 30° (a) and 60° (b), respectively ((1) $K_{T,}$ (2) K_G, (3) K_{ZT}, and (4) K_{ZG}).

the medium slope, and 0.23 and 0.25 for the steep slope. K_T are underestimated, and K_G are overestimated seriously in GOST2 because of the overestimation of canopy GF in GOST2.

The hotspot effect is an important phenomenon in canopy biophysical variable retrievals where the directions of view and sun coincide, and there is no shadow at the hotspot. From Figs. 6 and 7, the hotspot effects of K_T and K_G are captured well by GOFP-T. Both relative errors of K_T and K_G are less than $\pm 10\%$ at the hotspot (VZA $= -20°$) in both trees-on-slope models with three slopes in GOFP-T.

Four component area ratios show obvious slope effects: with increasing slope, K_T and K_{ZT} decrease in the backward-scattering direction and increase in the forward-scattering direction. On the contrary, K_G and K_{ZG} increase in the forward-scattering direction, and decrease with increasing slope in the backward-scattering direction. Both relative errors and RMSE of K_G between GOST2 and two 3-D models increase for SM with increasing slope, and decrease for HM. Increase in slope enhances the influence of tree distribution on four component area ratios at most VZAs for SM, especially for K_T and K_G. For HM, the slope effect enhances the influence of tree distribution in the forward-scattering direction. Yet, it weakens the tree distribution effect in the backward-scattering direction for HM with the steep slope. It means that the tree distribution also needs to be considered for forest plantations on the steep slope, especially in the forward-scattering direction.

Overall, the four component area ratios (especially for K_T and K_G) simulated in GOFP-T show high consistency with those in

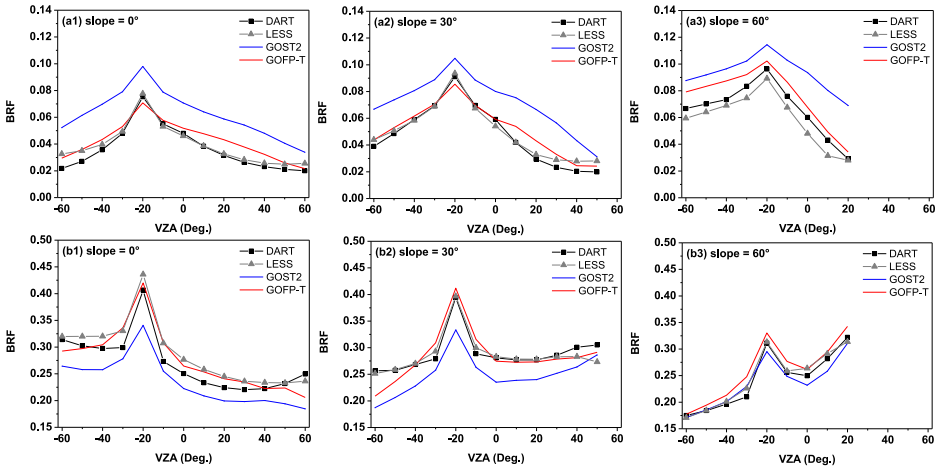

Fig. 8. Comparisons of canopy BRF in red (a) and NIR (b) bands among the four BRDF models in HM with slope = 0° (1), 30° (2), and 60° (3), respectively.

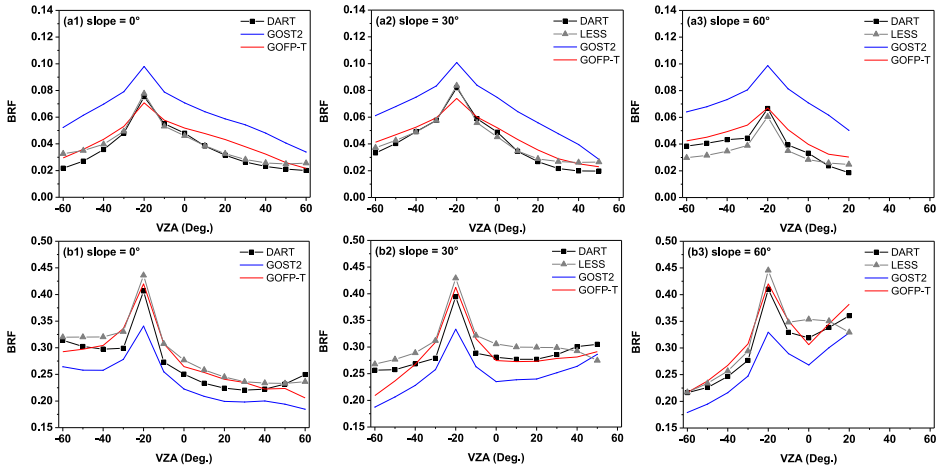

Fig. 9. Comparisons of canopy BRF in red (a) and NIR (b) bands among the four BRDF models in SM with slope = 0° (1), 30° (2), and 60° (3), respectively.

DART and LESS for both HM and SM. Large errors of four component area ratios can occur if the Poisson model is used to describe the tree distribution for forest plantations.

C. Canopy BRF

The comparisons of canopy BRF in the red and NIR bands among GOFP-T, GOST2, DART, and LESS are shown in Fig. 8 (HM) and Fig. 9 (SM).

Canopy BRF is closely related with the canopy four component area ratios The canopy BRF curve shapes in GOFP-T and GOST2 are similar to K_T variation in the NIR band (see Figs. 6 and 7), and they are similar to K_G variation in the red band. The main differences in the four component area ratios among the models result from the optical parameters of foliage and background used in the models. Canopy BRFs simulated with GOFP-T are consistent with DART and LESS in both red and NIR bands for HM and SM on three slopes. RMSE in BRF in the red band between GOFP-T and DART is only about 0.02 for both HM and SM on all slopes (except for the steep slope in HM, RMSE is 0.04). In the NIR band, RMSE is 0.04 and 0.11 for SMwith medium and steep slopes,, 0.06, 0.04 and 0.09 for HM on the three slopes, respectively. The hotspot effects of canopy BRF are captured well by GOFP-T in both red and NIR bands. The relative errors in BRF at the hotspot between GOFP-T and two 3-D BRDF models are less than $\pm 10\%$. Yet, compared with GOFP-T, GOST2 simulations show obvious deviation from DART and LESS simulations. Canopy BRFs simulated with GOST2 are seriously overestimated in the red band, and obviously underestimated in the NIR band at most VZAs. The primary reason is closely related to unrealistic description of tree distribution for forest plantations in GOST2, leading to the deviated simulation of canopy GF and four component area ratios. In addition, as the foliage reflectance is less than background reflectance in the red band and larger than background reflectance in the NIR band, serious underestimation of K_T and overestimation of K_G in GOST2 lead to the serious overestimation of BRF in the red band and underestimation in the NIR band.

Similarly, canopy BRF shows the slope effect in both trees-on-slope models, especially in the NIR band: with increasing slope, BRF decreases in the backward-scattering direction and

increase in the forward-scattering direction in the NIR band. On the contrary, it increases in the backward-scattering and decreases in the backward-scattering direction in the red band. The results are mainly due to the variation of K_T and K_G with slope (as shown in Figs. 6 and 7).

The deviations of BRF in GOST2 from DART and LESS are obvious for SM on all three slopes. For HM, GOFP-T simulations show high consistency with DART and LESS simulations on slope $= 0°$ and 30° in both red and NIR bands. When slope reaches up to 60°, the differences in canopy BRF in the NIR band among the four BRDF models are not obvious for HM. It is due to the deviation of K_T between GOST2 and LESS decreases on steep slopes. Yet, the difference in canopy BRF in the red band between the GOST2 and DART is non-negligible because of the deviation of K_G between GOST2 and LESS is obvious, especially in the forward-scattering direction.

Overall, the canopy BRF simulations in GOFP-T with the hypergeometric model are consisted with DART and LESS for both HM and SM. Compared with GOFP-T, canopy BRF simulated with GOST2 with the Poisson model is seriously overestimated in the red band, and underestimated in the NIR band, especially for SM. The results are due to the differences in canopy canopy GF and four component area ratios between GOFP-T and GOST2.

D. Compared With the Field Measurement

A pure forest stand (42°23'47"N, 117°22'19"E) with 100 m × 100 m was selected from Saihanba forest center, which is the largest forest plantations in Asia. The high resolution images (0.2 m × 0.2 m) and point cloud dataset was aquired on an airborne LiDAR LiCHy system from September 5 to 17, 2018. Point cloud dateset was processed: digital elevation model (i.e., slope and aspect), tree position, mean tree height, mean crown radius, and forest classified results were extracted from Lidar360 software (see Fig. 10). Leaf and background optical properties were measured with spectrograph. Crown height and LAI were measured through destructive sampling from three representative trees. Corresponding Landsat 8 OLI surface reflectance was acquired.[4]

The comparisons of tree distribution between measurement and simulations with GOFP-T and GOST2 are shown in Fig. 11. Both the measurement and simulations with GOFP-T show tall-thin shapes, while the Poisson simulation shows obvious wider distribution patterns. The simulations with GOFP-T show high consistency with the measurement, meaning that the tree distribution meets the hypergeometric model rather than the Poisson model in the forest stand.

After denoising, the forest coverage was obtained from the point clouds according to their vertical coordinates and cluster characteristics. The forest coverage in the stand is about 68%, which is close to the GOFP simulation (67%) in Table II. On contrast, the simulation in GOST2 (42%) with the Poisson model strongly underestimated. In addition, the underestimation

[4][Online]. Available: https://developers.google.com/earth-engine/datasets/catalog/LANDSAT_LC08_C01_T1_SR#description

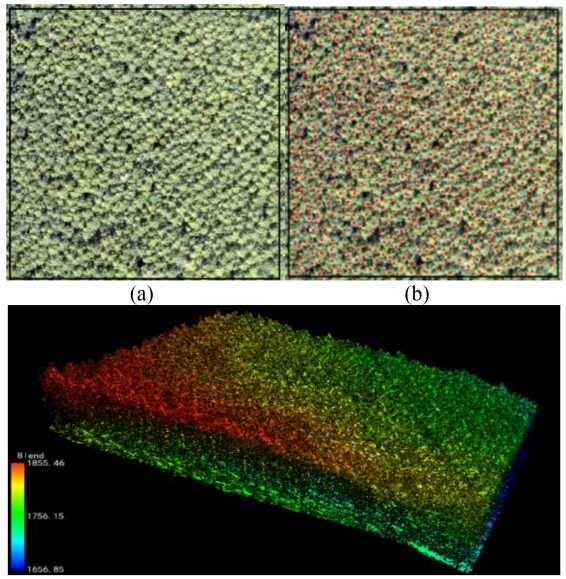

Fig. 10. Selected forest stand in a 100 × 100 m^2 sample plot. (a) High resolution image. (b) Crown positions (red points). (c) Point cloud.

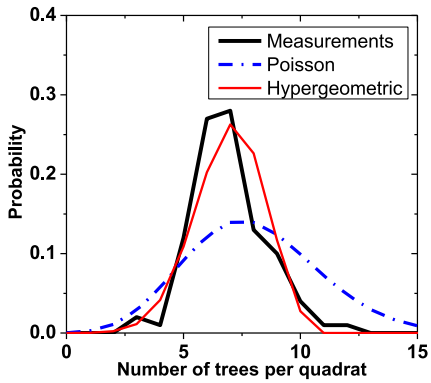

Fig. 11. Tree distribution in the selected plantation stand divided in 100 quadrats compared with the Poisson and hypergeometric distributions.

TABLE II
COMPARISONS OF FOREST COVERAGE AND CANOPY REFLECTANCE IN THE RED AND NIR BANDS BETWEEN SIMULATIONS AND FIELD MEASUREMENT

	GOFP-T	GOST2	Measurement*
Coverage (%)	67	49	68
Red	0.029	0.034	0.030
NIR	0.235	0.209	0.228

*Forest coverage measured with the LiDAR LiCHy system, and canopy reflectance measured with the Landsat8 OLI image.

of forest coverage in GOST2 leads to the inaccurate canopy reflectance simulation in the forest plantation stand. The simulations of canopy reflectance in two GO models are compared with the Landsat 8 OLI surface reflectance products. Although all view zenith angles in OLI images are almost the same, the nadir is the most important direction for many sensors. Canopy reflectance in GOST2 is overestimated by 13.7% in the red band, and underestimated 8.2% in the NIR band. While

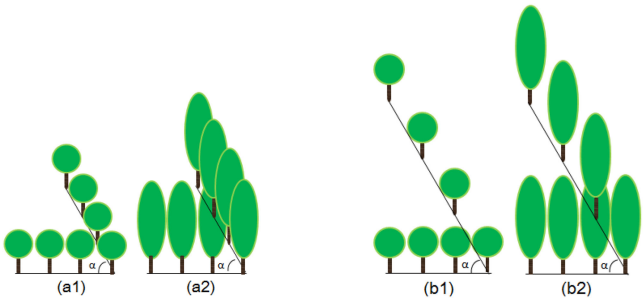

Fig. 12. Applicability of two trees-on-slope models. (a) SM: parameters on slope do not change with slope; (b) HM: parameters projected on horizontal ground do not change with slope.

the GOFP-T show high consistency with the Landsat 8 OLI surface reflectance product by correcting the tree distribution in the forest plantations: the relative error of canopy reflectance between GOFP-T and measurement is only -3.0% and 3.3% in the red band and NIR band, respectively.

V. Discussions

The results in this article show high performance in GOFP-T compared with GOST2. The errors in GOST2 simulations (e.g., canopy GF, K_T, K_G, and BRF) result mostly from the unrealistic description of tree distribution for forest plantations in GOST2. As GOFP-T combined the hypergeometric model with GOST2 for forest plantations specially, it avoids the problem. However, the abilities of GOST2 in simulating canopy GF, four component area ratios, and BRF are positively shown in this article (except for the description of tree distribution in forest plantations) and previous studies [7], [18].

The hypergeometric model is a common distribution for forest plantations. The essence of the model is the use of the exclusion distance among crowns in calculation of canopy GF in the view and sun directions, four component area ratios, and canopy BRF, and the results of these calculations are quite different from the Poisson model. We deem that the hypergeometric model is an advanced and practical model to describe the tree distribution for forest plantations relative to the Poisson model. It can be embedded or used in most GO models because canopy GF is a fundamental attribution of nearly all GO models.

A. Trees-On-Slope Models

Two commonly used trees-on-slope models (HM and SM) are described and compared in this article. There is no obvious difference between them for gentle and medium slopes (e.g., slope $\leq 30°$). While, the difference increases with increasing slope. Especially for the steep slope (e.g., slope $= 60°$), the sloping distance among crowns increases significantly because the sloping surface area is the horizontal surface area divided by cosine of slope (α) for HM.

Both HM and SM have their advantages, and have been used in previous studies: for SM, the horizontal distance among trees decrease with increasing slope, leading to the serious overlaps among crowns for thin-tall crowns [see Fig. 12(a)]. For HM, the sloping distances among crowns increases with increasing slope, leading to the significant increases in gaps among crowns [see Fig. 12(b)]. We deem that both overlaps [see Fig. 12(a2)] and gaps among crowns [see Fig. 12(b1)] are not quite realistic for forest plantations because there are often reasonable exclusion distances among crowns in forest plantations in reality. We deem that HM is suitable for tall and thin (such as tall cylinders) crowns, while SM is suitable for spherical or umbellate crowns, and for shrubs. From this perspective, there is no essential difference between these two trees-on-slopemodels because reasonable growth space of crowns on sloping terrains is considered in both models, although there are obvious differences in GF, four component area ratios, and BRF between these two models on the steep slopes. The abovementioned space or distance among crowns is the essence of the hypergeometric model but is not considered in the Poisson model.

B. Particular Tree Distributions

The hypergeometric model used in this article includes both regularity and randomness of tree distribution for forest plantations. It is a probability model that the tree position in a stand is of randomness. Some particular tree distributions, such as grid-shaped and line-shaped distributions for plantations or orchards have been studied [35], [39]. These distributions need some other parameters to describe the spatial relationship among crowns, e.g., grid size for grid-shaped distributions, line spacing for line-shaded distributions. In addition, the observation is dependent on azimuths of view and stand for a specific stand, because of the obvious difference in canopy GF among different view azimuths. These parameters inevitably increase the model complexity. Strictly speaking, these particular distributions are not described with probability statistics because the tree positions, mean and variance of tree number in a sample are relatively fixed values but not a probability. For these particular situations, we admit the hypergeometric model cannot replace these distributions completely. While, understandably, overlaps among crowns in the hypergeometric model are similar to those in the two particular models at low VZAs, resulting in no obvious differences in canopy GF, four component area ratios, and BRF between the hypergeometric model and these particular models. The main difference exists at larger VZAs and some particular azimuths (such as 0° and 90°), where overlaps among crowns in these models may be different from those produced by the hypergeometric model. Except in those cases, we deem that there are no obvious differences in canopy GF and BRF between the hypergeometric model and these particular distributions. The latter distributions may be regarded as specific cases of the hypergeometric model in this article.

VI. Conclusion

Tree distributions in forest plantations show obvious different spatial patterns from those in natural forests. Many studies showed that the influences of tree distribution and slope on canopy GF and BRF are non-negligible. In this article, GOFP with the hypergeometric model for horizontal surfaces was modified to form GOFP-T for sloping terrains to simulate canopy GF, four component area ratios, and BRF in two trees-on-slope

models (SM and HM) for forest plantations. Two 3-D radiative transfer models (LESS and DART) were used to compare and evaluate the simulations of GOFP-T. Results show that canopy GF, four component area ratios, and BRF simulated by GOFP-T shave show high consistency with these in two 3-D models. In addition, the simulations of canopy coverage and reflectance in GOFP-T compare well with the field measurements, meaning GOFP-T has ability in simulating the abovementioned parameters for forest plantations on sloping terrains. GOFP-T with the hypergeometric model in this article is a simple and new model for simulating canopy GF and BRF for forest plantations on sloping terrains with the consideration of exclusion distances among crowns. It is useful for comprehending remote sensing signals from forest plantations on sloping terrains for the purpose of parameter retrievals.

Acknowledgment

The authors would like to thank Dr. Y. Wang, Q. Zhan, J. Huang, and X. Qu for helpful discussions.

References

[1] T. Pillay and D. Ward, "Spatial pattern analysis and competition between Acacia Karroo trees in humid savannas," *Plant Ecol.,* vol. 213, no. 10, pp. 1609–1619, 2012, doi: 10.1007/s11258-012-0115-4.

[2] A. J. Larson and D. Churchill, "Tree spatial patterns in fire-frequent forests of western North America, including mechanisms of pattern formation and implications for designing fuel reduction and restoration treatments," *Forest Ecol. Manag.*, vol. 267, pp. 74–92, 2012, doi: 10.1016/j.foreco.2011.11.038.

[3] M. Yokozawa, Y. Kubota, and T. Hara, "Effects of competition mode on spatial pattern dynamics in plant communities," *Ecol. Model.*, vol. 106, no. 1, pp. 1–16, 1998, doi: 10.1016/S0304-3800(97)00181-6.

[4] P. Legendre and M. J. E. Fortin, "Spatial pattern and ecological analysis," *Vegetatio*, vol. 80, no. 2, pp. 107–138, 1989, doi: 10.1007/BF00048036.

[5] J. Geng *et al.*, "GOFP: A geometric-optical model for forest plantations," *IEEE Trans. Geosci. Remote Sens.*, vol. 55, no. 9, pp. 5230–5241, Sep. 2017, doi: 10.1109/TGRS.2017.2704079.

[6] J. Geng *et al.*, "Influence of the exclusion distance among trees on gap fraction and foliage clumping index of forest plantations," *Trees*, vol. 30, no. 5, pp. 1683–1693, 2016, doi: 10.1007/s00468-016-1400-y.

[7] S. Wu *et al.*, "Modeling discrete forest anisotropic reflectance over a sloped surface with an extended GOMS and SAIL model," *IEEE Trans. Geosci. Remote Sens.*, vol. 57, no. 2, pp. 944–957, Feb. 2019, doi: 10.1109/TGRS.2018.2863605.

[8] A. Rosema, W. Verhoef, H. Noorbergen, and J. J. Borgesius, "A new forest light interaction model in support of forest monitoring," *Remote Sens. Environ.*, vol. 42, no. 1, pp. 23–41, 1992, doi: 10.1016/0034-4257(92)90065-R.

[9] X. Li and A. H. Strahler, "Modeling the gap probability of a discontinuous vegetation canopy," *IEEE Trans. Geosci. Remote Sens.*, vol. 26, no. 2, pp. 161–170, Mar. 1988.

[10] X. Li and A. H. Strahler, "Geometric-optical bidirectional reflectance modeling of a conifer forest canopy," *IEEE Trans. Geosci. Remote Sens.*, vol. GE-24, no. 6, pp. 906–919, Nov. 1986.

[11] X. Li and A. H. Strahler, "Geometric-optical modeling of a conifer forest canopy," *IEEE Trans. Geosci. Remote Sens.*, vol. GE-23, no. 5, pp. 705–721, Sep. 1985.

[12] J. M. Chen and S. G. Leblanc, "A four-scale bidirectional reflectance model based on canopy architecture," *IEEE Trans. Geosci. Remote Sens.*, vol. 35, no. 5, pp. 1316–1337, Sep. 1997.

[13] S. G. Leblanc, P. Bicheron, J. M. Chen, M. Leroy, and J. Cihlar, "Investigation of directional reflectance in boreal forests with an improved four-scale model and airborne POLDER data," *IEEE Trans. Geosci. Remote Sens.*, vol. 37, no. 3, pp. 1396–1414, May 1999.

[14] T. Nilson, "Inversion of gap frequency data in forest stands," *Agricultural Forest Meteorol.*, vol. 98, pp. 437–448, 1999, doi: 10.1016/S0168-1923(99)00114-8.

[15] A. Kuusk, T. Nilson, M. Paas, M. Lang, and J. Kuusk, "Validation of the forest radiative transfer model FRT," *Remote Sens. Environ.*, vol. 112, no. 1, pp. 51–58, 2008, doi: 10.1016/j.rse.2006.06.025.

[16] A. Kuusk, "A fast, invertible canopy reflectance model," *Remote Sens. Environ.*, vol. 51, no. 3, pp. 342–350, 1995, doi: 10.1016/0034-4257(94)00059-V.

[17] X. Wang, G. Zheng, Z. Yun, and L. M. Moskal, "Characterizing tree spatial distribution patterns using discrete aerial lidar data," *Remote Sens.-Basel*, vol. 12, no. 4, pp. 712, 2020, doi: 10.3390/rs12040712.

[18] W. Fan, J. Li, and Q. Liu, "GOST2: The improvement of the canopy reflectance model GOST in separating the sunlit and shaded leaves," *IEEE J. Sel. Topics Appl. Earth Observ. Remote Sens.*, vol. 8, no. 4, pp. 1423–1431, Apr. 2015, doi: 10.1109/JSTARS.2015.2413994.

[19] J. Geng *et al.*, "Evaluation of GOFP over four forest plots using RAMI and UAV measurements," *Int. J. Digit. Earth*, vol. 14, pp. 1433–1451, 2021, doi: 10.1080/17538947.2021.1936226.

[20] G. Yin *et al.*, "Path length correction for improving leaf area index measurements over sloping terrains: A deep analysis through computer simulation," *IEEE Trans. Geosci. Remote Sens.*, vol. 58, no. 7, pp. 4573–4589, Jul. 2020, doi: 10.1109/TGRS.2019.2963366.

[21] B. Cao *et al.*, "Comparison of five slope correction methods for leaf area index estimation from hemispherical photography," *IEEE Geosci. Remote Sens. Lett.*, vol. 12, no. 9, pp. 1958–1962, Sep. 2015, doi: 10.1109/LGRS.2015.2440438.

[22] W. Fan, J. M. Chen, W. Ju, and G. Zhu, "GOST: A geometric-optical model for sloping terrains," *IEEE Trans. Geosci. Remote Sens.*, vol. 52, no. 9, pp. 5469–5482, Sep. 2014, doi: 10.1109/TGRS.2013.2289852.

[23] E. María LuisaB. Frédéric and W. Marie, "Slope correction for LAI estimation from gap fraction measurements," *Agricultural Forest Meteorol.*, vol. 148, no. 10, pp. 1553–1562, 2008, doi: 10.1016/j.agrformet.2008.05.005.

[24] W. Verhoef and H. Bach, "Coupled soil–leaf-canopy and atmosphere radiative transfer modeling to simulate hyperspectral multi-angular surface reflectance and TOA radiance data," *Remote Sens. Environ.*, vol. 109, no. 2, pp. 166–182, 2007, doi: 10.1016/j.rse.2006.12.013.

[25] B. Combal, H. Isaka, and C. Trotter, "Extending a turbid medium BRDF model to allow sloping terrain with a vertical plant stand," *IEEE Trans. Geosci. Remote Sens.*, vol. 38, no. 2, pp. 798–810, Mar. 2000, doi: 10.1109/36.842009.

[26] J. L. Widlowski *et al.*, "The fourth radiation transfer model intercomparison (RAMI-IV): Proficiency testing of canopy reflectance models," *J. Geophys. Res.,* vol. 118, no. 13, pp. 6869–6890, 2013.

[27] C. B. Schaaf, X. Li, and A. H. Strahler, "Topographic effects on bidirectional and hemispherical reflectances calculated with a geometric-optical canopy model," *IEEE Trans. Geosci. Remote Sens.*, vol. 32, no. 6, pp. 1186–1193, Nov. 1994.

[28] G. Yin, A. Li, W. Zhao, H. Jin, J. Bian, and S. Wu, "Modeling canopy reflectance over sloping terrain based on path length correction," *IEEE Trans. Geosci. Remote Sens.*, vol. 55, no. 8, pp. 4597–4609, Aug. 2017, doi: 10.1109/TGRS.2017.2694483.

[29] Y. Wang and J. Gastellu-Etchegorry, "Accurate and fast simulation of remote sensing images at top of atmosphere with DART-Lux," *Remote Sens. Environ.*, vol. 256, 2021, Art. no. 112311, doi: 10.1016/j.rse.2021.112311.

[30] X. Li, A. H. Strahler, and C. E. Woodcock, "A hybrid geometric optical-radiative transfer approach for modeling albedo and directional reflectance of discontinuous canopies," *IEEE Trans. Geosci. Remote Sens.*, vol. 33, no. 2, pp. 466–480, Mar. 1995.

[31] J. Qi *et al.*, "LESS: Large-scale remote sensing data and image simulation framework over heterogeneous 3D scenes," *Remote Sens. Environ.*, vol. 221, pp. 695–706, 2019, doi: 10.1016/j.rse.2018.11.036.

[32] J. P. Gastellu-EtchegorryE. Martin and F. Gascon, "DART: A 3D model for simulating satellite images and studying surface radiation budget," *Int. J. Remote Sens.*, vol. 25, no. 1, pp. 73–96, 2004.

[33] J. P. GastelluEtchegorry, V. Demarez, V. Pinel, and F. Zagolski, "Modeling radiative transfer in heterogeneous 3-D vegetation canopies," *Remote Sens. Environ.*, vol. 58, no. 2, pp. 131–156, 1996, doi: 10.1016/0034-4257(95)00253-7.

[34] J. Widlowski *et al.*, "The fourth phase of the radiative transfer model intercomparison (RAMI) exercise: Actual canopy scenarios and conformity testing," *Remote Sens. Environ.*, vol. 169, pp. 418–437, 2015, doi: 10.1016/j.rse.2015.08.016.

[35] J. L. Widlowski *et al.*, "The RAMI on-line model checker (ROMC): A web-based benchmarking facility for canopy reflectance models," *Remote Sens. Environ.*, vol. 112, no. 3, pp. 1144–1150, 2008, doi: 10.1016/j.rse.2007.07.016.

[36] B. Pinty *et al.*, "Radiation transfer model Intercomparison (RAMI) exercise: Results from the second phase," *J. Geophys. Res.*, vol. 109, 2004, Art. no. D06210D6, doi: 10.1029/2003JD004252.
[37] B. Cao *et al.*, "A general framework of kernel-driven modeling in the thermal infrared domain," *Remote Sens. Environ.*, vol. 252, 2021, Art. no. 112157, doi: 10.1016/j.rse.2020.112157.
[38] Z. Bian *et al.*, "Modeling the directional anisotropy of fine-scale TIR emissions over tree and crop canopies based on UAV measurements," *Remote Sens. Environ.*, vol. 252, 2021, Art. no, 112150, doi: 10.1016/j.rse.2020.112150.
[39] J. M. Norman, "Radiative transfer in an array of canopies," *Agronomy J.*, vol. 75, no. 3, pp. 481–488, 1983, doi: 10.2134/agronj1983.00021962007500030016x.

Jun Geng received the M.S. degree in ecology from Nanjing Forestry University, Jiangsu, China, in 2012 and the Ph.D. degree in geography from Nanjing University, Nanjing, China, 2016.

He is currently a Lecturer with the Hefei University of Technology, China. His research interests include canopy reflectance modeling, remote sensing modeling, and applications for vegetation ecosystem.

Jing M. Chen (Senior Member, IEEE) received the Ph.D. degree in meteorology from Reading University, Reading, U.K., in 1986.

He is currently a Professor with the Department of Geography and Program in Planning, University of Toronto, Toronto, ON, Canada; a Canada Research Chair; and a Fellow of the Royal Society of Canada. He is a professor with Fujian Normal University, Fuzhou, China. He has authored and coauthored more than 200 papers in refereed journals, which have been cited more than 5000 times in the scientific literature. His major research interests include remote sensing of vegetation and quantifying terrestrial carbon and water fluxes.

Dr. Chen is currently an Editor-in-Chief of *Remote Sensing of Environment*, and Associate Editor of *Journal of Geophysical Research-Atmosphere*, *Canadian Journal of Remote Sensing,* and *Journal of Applied Remote Sensing*.

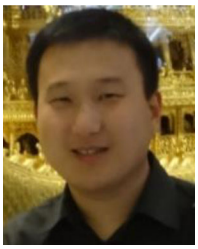

Weiliang Fan (Member, IEEE) received the B.S. degree in horticulture from Shandong Agricultural University, Shandong, China, in 2007, the M.S. degree in forest management from Zhejiang A&F University, Zhejiang, China, in 2010, and the Ph.D. degree in geography from Nanjing University, Nanjing, China, in 2013.

He is currently an Associate Professor with Zhejiang A&F University, China. His research interests include canopy reflectance modeling and applications for vegetation ecosystem.

Lili Tu received the M.S. degree from Nanjing University, Jiangsu, China, in 2012, and the Ph.D. degree in geography from Nanjing University, Nanjing, China, in 2017.

She is currently a Lecturer with Anhui Agricultural University, China. Her research interests include multiangle remote sensing, applications for vegetation ecosystem, and the application of thermal infrared remote sensing.

Yong Pang received the B.S. degree in forestry from Anhui Agriculture University, Hefei, China, in 1997, the M.Agr. degree in forest management from the Chinese Academy of Forestry, Beijing, China, in 2000, and the Ph.D. degree in cartography and geography information system from the Chinese Academy of Sciences, Beijing, China, in 2006.

From 2006 to 2008, he was a Postdoctoral Researcher with the Department of Forest, Rangeland, and Watershed Stewardship, Colorado State University, Fort Collins, CO, USA. He is currently a Professor with the Research Institute of Forest Resource Information Techniques, Chinese Academy of Forestry. His research interests include surface height and vegetation spatial structure from InSAR and light detection and ranging (LiDAR), modeling of LiDAR waveforms from forest stands, and development of algorithms for forest parameter retrieval from remote sensing data.

Gang Yuan received the B.S. degree in surveying engineering in 2020 from Hefei University of Technology, Anhui, China, where he is currently working toward the M.S. degree in surveying engineering.

His research interests include canopy modeling and machine learning.

Lichen Xu received the B.S. degree in surveying engineering from Anhui Jianzhu University, Anhui, China, in 2019. He is currently working toward the M.S. degree in surveying engineering with Hefei University of Technology, Anhui, China.

His research interests include big data processing and machine learning.

Canyang Zhu received the B.S. degree in surveying engineering from Nanjing Forestry University, Jiangsu, China, in 2020. She is currently working toward the M.S. degree in surveying engineering with Hefei University of Technology, Anhui, China.

Her research interests include canopy modeling and machine learning.

Teng Zhang received the B.S. degree in geographic information system (GIS) from Lanzhou Jiaotong University, Lanzhou, China, in 2021. He is currently working toward the M.S. degree in surveying engineering with Hefei University of Technology, Anhui, China.

His research interests include canopy modeling and LiDAR point cloud processing.

Chunju Zhang received the Ph.D. degree in cartography and geographic information system from the School of Geographical Science, Nanjing Normal University, Nanjing, China, in 2013.

She is an Associate Professor with the School of Civil Engineering, Hefei University of Technology, Hefei, China. Her research interests include computational intelligence in remote sensing images and geographic knowledge graph.

Zhourun Ye was born in Anhui, China. He received the B.S. degree in geomatics engineering from Liaoning Technical University, Liaoning, China, in 2007, and the M.S. and Ph.D. degrees in geodesy and geomatics engineering from the University of Chinese Academy of Sciences, Beijing, China, in 2010 and 2015, respectively.

He was a Visiting Ph.D. Student with the University of Stuttgart, Stuttgart, Germany, for 24 months, i.e., from November 2012 to October 2014.

Yongchao Zhu was born in Hubei, China. He received the B.S. and M.S. degrees in geomatics engineering and the Ph.D. degree in geodesy and geomatics engineering from Wuhan University, Wuhan, China, in 2012, 2014, and 2018, respectively.

He was a Visiting Ph.D. Student with German Research Center for Geosciences GFZ for 18 months, i.e., from January 2017 to July 2018. He is currently with the College of Civil Engineering, Hefei University of Technology, China. His research interests include ocean and land remote sensing applications using GNSS-reflectometry techniques.

Zhenxuan Li received the Ph.D. degree in geodesy and surveying engineering from the China University of Mining and Technology, Xuzhou, China, in 2018.

He is currently a Lecturer with the School of Civil Engineering, Hefei University of Technology, Hefei, China. His research interests include disaster remote sensing and ground feature change detection based on remote sensing image.